Towards more precise estimates of land-use requirements for solar photovoltaic power plants

Damien Vermeer

Middleton Group, Melbourne (Australia)

Abstract

There is a lack of PV module rating agnostic research in solar PV power plant land use requirements. Existing literature focuses on peak capacity (watts) or energy (watt-hours) per unit area, which limits the validity of the results as the age from publication increases due to the rapid (and ongoing) increase in PV module performance.

The aim of this paper is to derive a relationship for the Ground Coverage Ratio (GCR, ratio of total solar PV module area to total land area) of a single-axis solar PV power plant to be used as an accurate, yet simple, model for land use prediction.

In this paper, a toolkit was created using the Python programming language to create a solar PV power plant layout, given a land parcel polygon selected from actual (scaled) cadastral land boundaries in Victoria, Australia.

Approximately 200,000 solar PV power plant layouts were simulated across 8 permutations of design criteria. Whilst no clear correlation was found between any land parcel properties and the GCR, all permutations indicated a relatively uniform GCR which was highly correlated with the natural logarithm of the row spacing.

By deriving the land use requirements of single-axis solar PV power plants based on design principles such as row spacing, azimuth tolerance and perimeter setback – but not module capacity – the results of this paper remain relevant into the future even with increasing solar PV module capacity.

Keywords: Solar PV power plant, land-use, solar farm, spacing, area

1. Introduction

Recent years have seen the rapid development of large-scale solar photovoltaic (PV) power plants throughout the world. Given the focus on reducing the effects of global warming, analysis to deduce the required area to supply a state, province or country with large-scale solar PV power plants has become both more prevalent in the literature and of greater importance for industry and government throughout the globe.

2. Literature Review & Scope

A high-level review of the literature was completed to identify existing spatial requirements for large-scale solar PV power plants, which are summarized below. Note the units have been converted by the author to a common unit (W/m^2) where feasible to allow direct comparison.

- Denholm and Margolis (2008) calculated 48.0 Wdc/m^2 for a single-axis tracking solar PV power plants as part of a wider analysis.
- Hernandez et al (2013) analysed 57 existing and planned solar PV power plants and deduced a range of 29.7 W/m^2 to 35.0 W/m^2. 13 peer review studies were also reviewed, however significant variance in the data was observed.
- Ong et al (2013) calculated the capacity-weighted average of 55 existing single-axis tracking solar PV power plants in the USA as 28.4 W/m^2.
- Horner and Clark (2013) condensed a wide range of studies on land use requirements and concluded a land-use estimate range of 5-55 m^{2}y/MWh for various types of solar power plants, including solar PV and CSP.
- Wachs and Engel (2021) assessed 12 papers, identifying a range of land use requirements, but noted '*Land use efficiency for solar [PV] has increased dramatically due to technological improvements, and newer assessments are needed that take into account improved efficiency*'

doi:10.18086/swc.2021.37.08 Available at http://proceedings.ises.org

This point by Wachs and Engel is critical. All studies considered above derive land use efficiency based on peak capacity (W) or total power output (Wh), overlooking the critical factor of Ground Coverage Ratio (GCR) which is the ratio of total solar PV module capacity to total land area.

By concluding land requirements in terms of capacity or power, the results presented become less accurate as their age from publication increases, due to the rapid (and ongoing) increase in module performance and efficiency (Figure 1). A solar PV power plant installed in the future will almost certainly use higher efficiency panels than those installed previously, which in turn leads to an increase in power plant power output for the same area, resulting in lower land required for the same output capacity.

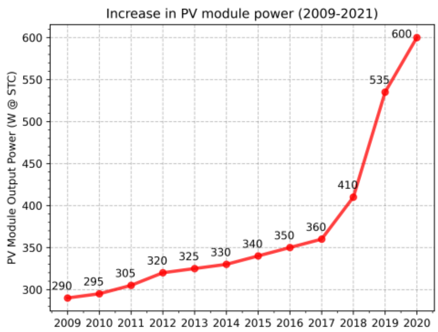

Fig. 1: Graph of historic solar PV module capacity growth since 2009, derived from Trina Solar data (2021).

Based on this common limitation, this paper presents a forward-looking study to deduce the land-use requirements of large-scale solar photovoltaic (PV) power plants from facility design principles, with the aim to derive a relationship for GCR which can be used into the future as solar module capacity continues to grow.

The remainder of this paper is structured as follows. Sections 3 and 4 describes the core design assumptions, based on Australian large-scale solar PV industry best practice design, which are used as inputs in Section 5 to a custom developed Python software package which generates a solar PV power plant layout. Section 6 discusses the results from this software package using land parcel data and deduces relationships to estimate power plant capacity for a given land size. Conclusions and future work are discussed in Section 7.

3. Assumptions – Solar Design

To focus the scope of this investigation, single-axis tracking solar PV systems similar to the below in Figure 2 have only been considered. This technology is used in multiple developed and planned large-scale solar PV power plants within Australia (ARENA, 2018).

Fig. 2: Single-axis solar PV power plant in Australia

Unfortunately, there are not (to the authors knowledge) any Australian, nor international, industry design practice guidelines from which to reference the design criteria for a single-axis tracking solar PV power plant. Instead, the author provides the following as assumptions for this analysis based on project design & development experience.

Solar power plants use solar modules (panels) with typical dimensions of ~1000 mm wide by ~2000 mm tall, typically installed in a portrait arrangement as per Figure 2 above. For this investigation we have assumed module dimensions of 1000 mm by 2000 mm.

Single-axis solar PV power plants feature a series of modules on a common structure. This structure is typically aligned towards the equator (though can be orientated away from true north/south within a small tolerance without a significant impact to power plant yield) and rotates east-west to track the sun. The number of modules per row structure varies but is commonly an integer multiple of the string length chosen by the designer. Row lengths of one string, two strings and three strings are the most common. Many modern Australian solar PV power plants use 1500 V_{DC} strings, meaning for a 'typical' solar module string lengths are usually in the range of 25 to 28 modules, with higher preferred due to lower copper losses in the DC cabling. For this investigation we have assumed 28 modules per string giving total row lengths of 32 m (1 string), 60 m (2 strings) and 88 m (3 strings) with an allowance of 4.0 m for supporting equipment such as slew motor, pier mounts and spacers.

The east-west spacing between row structures is typically selected by the power plant designer, but in the Australian market typically falls between 4.0 and 7.0 m ‘post-post’ (horizontal distance from middle of one row structure to the middle of the second). Lower spacing between row structures can cause interrow shading, reducing the specific yield (kWh / kWp / year) of the power plant but also increasing the peak output (kWac) of the power plant – effectively each module is less efficient but more fit modules overall. Maintenance access and common fire-fighting spacing requirements often lead to higher interrow spacing within Australia solar PV power plants. For this investigation we have considered interrow spacing between 4.0 to 7.0 m.

In the author’s experience, there are two common row layout design themes for solar PV power plants, ‘block’ alignment and ‘boundary edge’ alignment. Block alignment aims to create consistent blocks of rows (and an associated inverter station) which can be duplicated and is commonly used for extremely large solar PV power plants with ample available land area. Boundary edge alignment aims to use all available area by aligning the rows to the edge of the land area, typically creating irregular layouts. As boundary edge alignment typically gives a higher capacity than block alignment (as it aims to use all available land) it has been used in this investigation.

A setback from the property edge is common for large-scale solar PV power plants in Australia based on local fire-fighting requirements. A clear space of 10.0 m from the edge to the nearest module is common and thus for this investigation we have considered property edge setbacks from 0.0 to 10.0 m.

Access roadways are important for maintenance access for all large-scale solar PV power plants. Design criteria for roadways differ based on the facility owner’s requirements and local fire-fighting access requirements. A perimeter roadway within the fire-fighting exclusion zone is very common and has been included in this investigation whenever the perimeter setback is greater than 0 m. For this investigation, we assume internal horizontal roadways are provided at the end of every two rows of maximum length, meaning roadways are spaced within the facility approximately 200 m apart. We have also assumed that this roadway is contained within an 8.0 m clear section between the end of rows, with this space to be used for the roadway itself, inverter stations and cable trenches. In the author’s experience, this represents the minimum quantity of access roads required to allow efficient maintenance of the power plant.

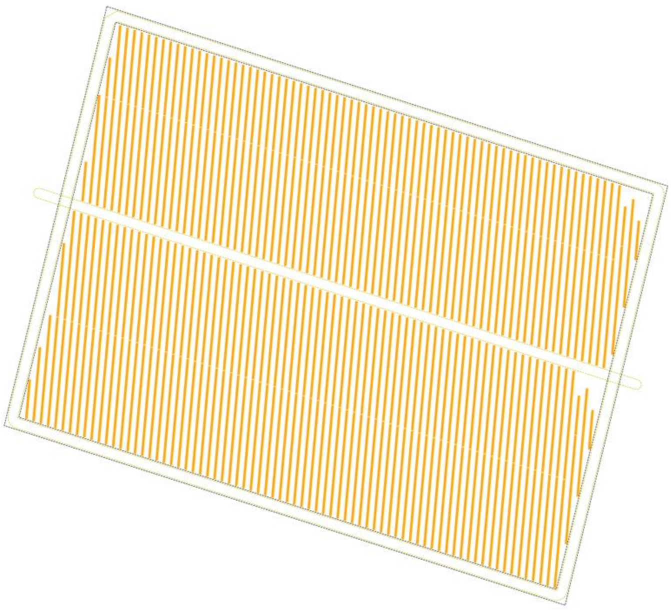

Fig. 3: Example solar PV power plant layout showing a single internal road (8.0 m clearway) and a perimeter road

Solar PV power plants typically require connection assets, such as collector switchgear and main transformer(s) to step-up the voltage to transmission level or otherwise. The location of these assets is commonly driven by the location of the nearest network asset (such as an overhead line or existing substation) rather than what the optimal location is for the asset based on the available land. For example, if the nearest connection point into the local network is an overhead line to the north-east of the site, the north-east corner of the available land is a good candidate for the location of these connection assets, as is a small piece of land just outside of the power plant land. Based on this restriction (unclear where, if at all, this asset should be located within the site) we have not included any spacing for connection assets in this investigation. This means this investigation may slightly under-estimate the land required for a given solar PV power plant.

Tab. 1: Assumed solar PV power plant design parameters for this investigation

Parameter	Varied during analysis?	Value	Notes
Module dimensions	No, fixed value	1000 mm x 2000 mm	
String length	No, fixed value	28 modules	To suit to 1500 V_{DC} inverters
Row type	No, fixed value	Single-axis single module (portrait) tracking system	Similar to Figure 2 above
Azimuth Tolerance	Yes	±5°, ±10°, ±15°	Allowable tolerance away from true north
Row lengths (3, 2 & 1 string)	No, fixed value	88.0, 60.0, 32.0 m	Assuming 4.0 m for row structure, motor, pier mounts and spacers
Row spacing	Yes	4.0, 5.0, 6.0, 7.0 m	Post-post spacing
Row alignment	No, fixed value	Boundary edge alignment	
Property boundary setback	Yes	0.0, 5.0, 10.0 m	
Perimeter access roadways	No, fixed value	Only if setback > 0.0m	
Internal access roadways	No, fixed value	8.0 m clearway east-west every ~200 m vertically	No vertical roadways
Spacing for connection assets in power plant	No, fixed value	Not included	

4. Assumptions – Land Area

In this section we discuss the assumptions on the land parcels used for this analysis.

For this investigation we have considered solar PV power plant facility layouts in only two dimensions, as full three-dimensional layout generation is complex. As solar PV facilities in Australia are predominantly developed on flat land, the variation between 2D and 3D analysis would likely be small and thus has been ignored in this study.

We have also assumed that each land parcel has no overlay restrictions (such as trees, waterways, locations of cultural or ecological significance etc) as attempting to parametrize this requirement without introducing substantial bias in the results is difficult.

To increase the validity of the results, the polygons representing the land area for the solar PV power plants were selected from the 'Vicmap Property' (2021) data set, which represents the cadastral boundaries of all land titles in the state of Victoria, Australia. Polygons representing the boundaries were extracted from the shapefile in the Vicmap Property database and scaled to a unit area for analysis prior to inclusion in the analysis dataset. The process is described below (summarized in Table 2) and was completed using the Python toolkit developed for this application, which is further discussed in Section 5.

Firstly, any polygons representing the available land area with self-intersections (Table 2, ref 1) or similar data quality errors (such as two areas connected by a very thin segment) were not added to the data set.

A land parcel which is skinny in one axis, yet wide in another, is typically not economically viable as a solar PV power plant due to the long DC and AC cables required. If extremely skinny in one axis, limitations on maximum row length can also be imposed which further prohibits economic viability (requires significantly more structures to install). As per Table 2 ref 2 below, these land parcels are excluded by a test which calculates the ratio of the length L_{MBB} to the width W_{MBB} of the minimum rotated rectangle (rotated bounding box) of the land parcel. Note the length L_{MBB} is defined as the longest side of the minimum rotated rectangle. If this value is greater than 3.0 the land parcel is not added to the data set.

Similarly, if the land is skinny in one axis and contains one or more segments (for example, an L shaped piece of land) it may not be economically viable to develop either. As per Table 2 ref 3 below, these land parcels are excluded by calculating the ratio of the area of the land parcel and the area of the minimum rotated rectangle. If the value is less than 0.1 the land parcel is not added to the data set.

Finally, prior to adding the land parcel to the analysis dataset, the raw land parcel is compared to all other land parcels already in the analysis dataset. If each vertex of the land parcel polygon is within 0.05 units (for the scaled polygon) of a corresponding vertex on a land parcel in the data set, it is not included. This is to avoid introducing bias in the results by adding multiple similar land parcels. Refer to Table 2 ref 4 below.

Tab. 2: Assumed solar PV power plant design parameters for this investigation

Ref	Name	Calculation	Skipped if	Example of polygon which is <u>not</u> added to dataset
1	Self-intersection or Fragmented	N/A	Detected	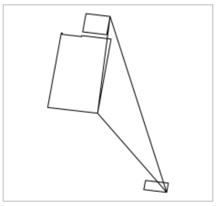
2	Land aspect ratio	$\frac{L_{MRR}}{W_{MRR}}$	> 3.0	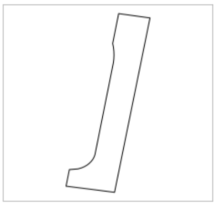
3	Minimum rotated rectangle area ratio	$\frac{A_{Land}}{A_{MRR}}$	< 0.1	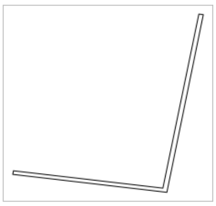
4	Polygon similarity	N minimum distances	< 5.0 %	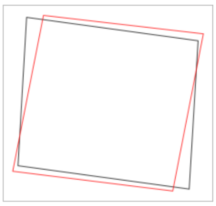

Using the above process, a subset of 500 polygons was selected. To further reduce land parcel bias, the polygon area and rotation was linearly scaled throughout the entire dataset. Final land parcel areas ranged from 30,000 m^2 to 550,000 m^2, which is approximately equivalent to 1.0 to 20.0 MWac assuming the upper range of 35 W/m2 calculated by Hernandez et al (2013). This area band was specifically selected to strike a balance between reasonable simulation time whilst maintaining feasibility of extrapolating the results to much larger solar PV power plants.

To visually confirm if there was any clear polygon bias in the data set, the polygons were scaled to area of one and plotted with aligned centroids and high transparency using Python. Bias to a particular shape or orientation of land would appear as a bold line or series of lines, which were not observed as per Figure 4 below.

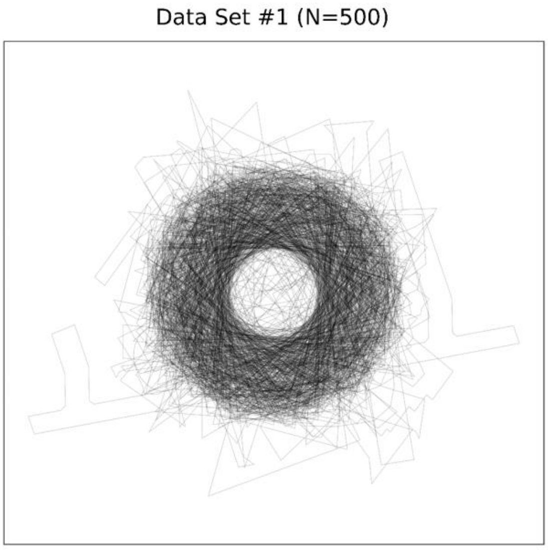

Fig. 4: Centroid aligned unit area scaled polygons within data set plotted with high transparency. No duplicates of the same shape on the same rotational axis can be seen (would appear as bold, distinct lines). Concentration of polygon boundaries into an annulus is likely caused by the unit scaling of the polygon boundaries.

5. Solar PV Power Plant Layout in Python & Method

In this section we discuss the method used of deriving the solar PV power plant layout given the design criteria discussed in Section 3 and the land parcels selected in Section 4.

A toolkit was developed for this project in Python and is publicly available (see Section 7). The toolkit uses multiple Python libraries such as *shapely* (polygon & planar feature analysis), *matplotlib* and *seaborn* (plotting), *numpy* (numerical analysis), *statsmodels* (statistics & curve fitting) and *pyshp* (shapefile library).

The base toolkit creates a solar PV power plant layout based on design criteria like that discussed in Section 3. Design optimization can be achieved by iterating over design values (such as azimuth, row spacing etc) and rerunning the algorithm. For this investigation, the design optimization target was to achieve the highest number of modules on the site.

Up to 50 different design permutations were calculated for each of the 500 land parcels. This process was repeated 8 times to investigate the impact of row spacing, allowable azimuth tolerance and perimeter setback, giving an approximate total of 200,000 simulations being completed.

Data describing the resulting solar PV power plant was recorded for the best result (highest number of modules) from the 50 design permutations.

A total of 8 separate iterations (sequences of 500 land parcel studies) were completed and summarised in Table 3 below. The results of these iterations are discussed in the next section.

Tab. 3: Summary of the 8 iterations completed in this investigation

Iteration #	Inter-row Spacing	Perimeter Offset	Azimuth Tolerance
1	6.0 m	10.0 m	±10°
2	7.0 m	10.0 m	±10°

Iteration #	Inter-row Spacing	Perimeter Offset	Azimuth Tolerance
3	5.0 m	10.0 m	±10°
4	4.0 m	10.0 m	±10°
5	6.0 m	5.0 m	±10°
6	6.0 m	0.0 m	±10°
7	6.0 m	10.0 m	±5°
8	6.0 m	10.0 m	±15°

An example of a 'best' layout (the highest number of modules from the 50 layouts generated for this land parcel for a given iteration) as generated by the toolkit is shown below.

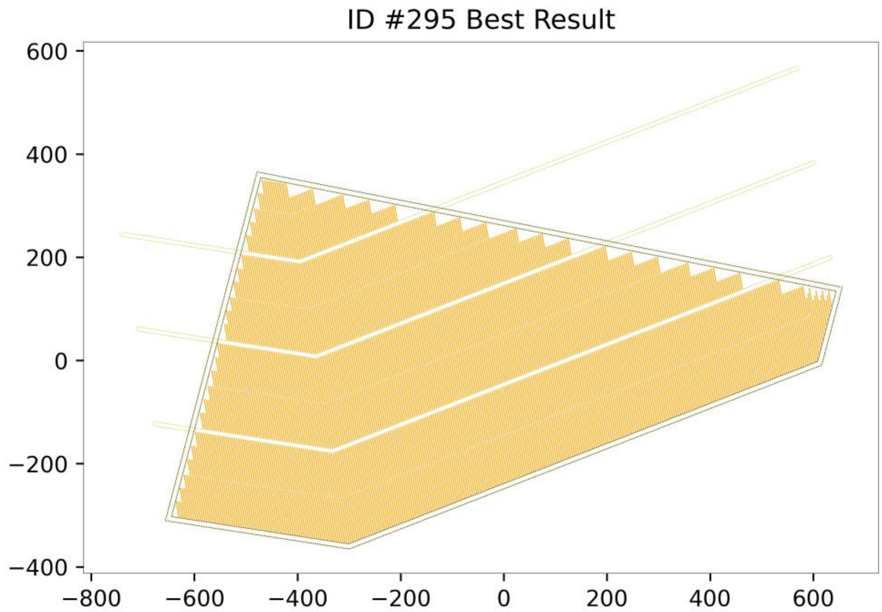

Fig. 5: Example 'best' layout (highest number of modules) generated by the brute-force optimisation algorithm for this land parcel polygon.

6. Results & Discussion

6.1 Definition of GCR

In this section we discuss the results of the Python simulations completed. As per Section 2, all results will be discussed in terms of Ground Coverage Ratio (GCR) which is the ratio of total solar module area to total available land area, as shown below.

$$GCR = \frac{N_{module} L_{module} W_{module}}{A_{Land}} \quad (1)$$

Where:

- N_{module} is the number of modules on the entire site
- L_{module} and W_{module} are the length and width of the module respectively (m)
- A_{Land} is the area of the land parcel (m^2)

Note occasionally solar PV power plant land use efficiency is described in terms of packing factor (pf) which is the reciprocal of GCR.

6.2 Analysis of Results

To begin our analysis, we will investigate single variable correlations between properties of the land parcel polygon and the calculated GCR for iteration #1 as per Table 3.

Tab. 4: Single variable linear correlations for iteration #1 as per Table 3. Refer to Table 2 for definitions of the independent variables used.

Independent Variable	**Dependent Variable**	**Linear R^2 Correlation**
Land area	GCR	< 0.1
Land aspect ratio		< 0.1
Minimum rotated rectangle area ratio		< 0.1

As shown above, all parameters tested show no linear correlation to GCR, indicating that they are not a useful predictor of GCR for any given land parcel. This was expected due to the significant variation in land parcel polygons which could give an identical area, aspect ratio or minimum rotated rectangle area ratio. Results of a similar magnitude were identified for the other iterations completed.

Several permutations of multivariate linear and non-linear correlations were considered for the independent variables above, but all showed weak correlation ($R^2 < 0.2$) and occasionally very large condition numbers, indicating potential multicollinearity in the results (which is likely, given polygon area and minimum rotated rectangle area ratio are somewhat related).

Analysis was then completed to determine the variability of the GCR within the results of a single iteration (500 land parcels). A box plot of the data (Figure 6, Left) of the GCR shows a very narrow 95% confidence band for the median in addition to a relatively narrow interquartile range. This implies that, although it appears hard to predict based on land parcel properties, the estimated GCR of any given land parcel appears relatively constant.

The analysis was then expanded to include variable post-post row spacing (iterations #1 through #4). As expected, the median GCR (Figure 6, Right) steadily increased with reducing interrow spacing. The interquartile range was relatively uniform, but upon visual inspection appears to be slightly positively correlated to the interrow spacing.

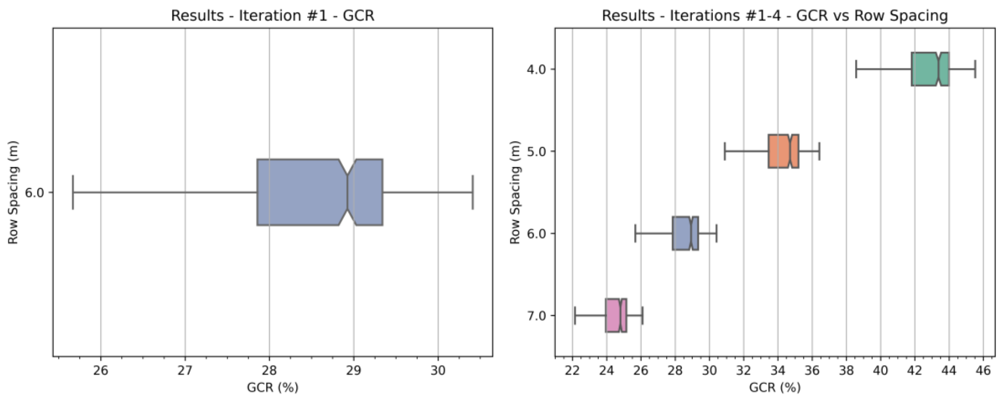

Fig. 6: (Left) Boxplot of results of iteration #1, showing relatively narrow 95% confidence interval for median and relatively narrow interquartile range.
(Right) Boxplot of results of iterations #1 through #4, showing non-linear increase in GCR for linear decrease in row spacing. Note vertical axis is reversed.

Iterations #1, #5 and #6 were then considered to investigate the effect of variable land parcel perimeter offset (Figure 7). No clear relationship was identified, however a small difference in the minimum and maximum values of the boxplots is likely attributed to the discrete nature of solar PV row structures – a small increase in available land may not allow additional modules, but the increase in available land corresponds to a decrease in GCR. This hypothesis is reinforced by the alignment of all median values for this study.

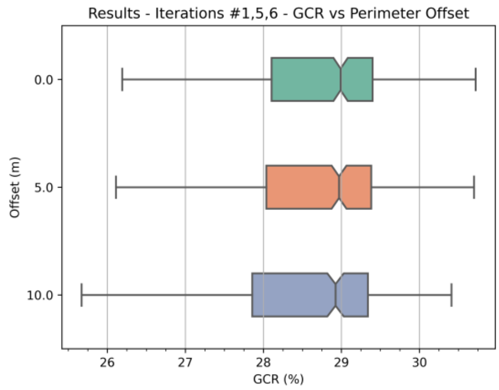

Fig. 7: Boxplot of results of iteration #1, #5 and #6 indicating no material variability or relationship between GCR and perimeter offset for a solar PV power plant.

Iterations #1, #7 and #8 were considered together to investigate the effect of allowable azimuth tolerance. To prevent giving an advantage to any one iteration and to allow direct comparison, the number of optimisation steps the brute-force algorithm could complete was identical between iterations #1, #7 and #8. An interesting relationship can be seen in Figure 8 below – a higher azimuth tolerance window (up to ±15° away from true north/south) resulted in lower variance to the GCR, but only marginally achieved a higher median than the other, lower, azimuth tolerances. This is likely as the layout algorithm can better align the module rows to the perimeter of the land parcel with higher azimuth tolerance.

Importantly, we note as azimuth angle increases away from true north (for the Southern Hemisphere) the specific yield of the solar PV power plant decreases due to the modules being orientated sub-optimally. This implies that a higher azimuth tolerance angle may not be preferred in a final solar PV power plant design compared to one with lower azimuth tolerance.

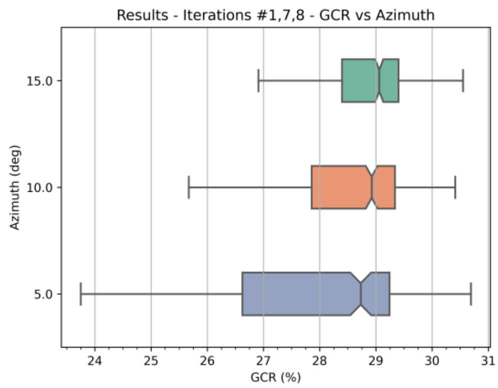

Fig. 8: Boxplot of results of iteration #1, #7 and #8 indicating the variability of GCR decreases with increasing azimuth tolerance.

To summarise the analysis completed:

- There was no reliable linear, multivariate linear or non-linear relationship identified between any of the land parcel parameters (area, aspect ratio or minimum rotated rectangle area ratio) and GCR.
- A strong non-linear relationship was identified between post-post row spacing and GCR.
- No relationship was identified between perimeter setback and GCR.
- Although the variance of GCR appeared correlated with the azimuth tolerance, the median GCR did not appear to be strongly correlated to azimuth tolerance.

6.3 Derivation of Models

Based on the above analysis, two results can be derived. Given the design and land parcel assumptions in Section 3 and 4 above and all iterations completed, Python was used to calculate the mean GCR, a 95% confidence interval for this mean and the standard deviation for the aggregate of all iterations (#1 through #8) completed.

If no prior knowledge is known about the land use parcel or the solar PV power plant desired (within the bounds of the assumptions in Section 3 and 4 above) the following mean GCR can be used.

Tab. 5: Derived mean GCR, confidence interval and standard deviation from the aggregate result of all iterations completed in this study.

GCR *Assuming no prior design/land knowledge*		
Mean	**95% confidence interval for mean**	**Standard deviation**
32.39%	32.08 – 32.70%	7.04

However, if the row spacing R is known (or selected) the accuracy of the estimation can be improved beyond a simple mean and standard deviation.

Based on Figure 6 (right) above, we can see a clear non-linear relationship between row spacing and the median GCR. Using least squares regression in Python, the natural logarithm of the row length independent variable was used to deduce a very strong relationship (Figure 9). Iterations #1 through #4 were only used in the calculation of this line of best fit to prevent over-weight of the row length = 6.0 m condition (iterations #5 through #8).

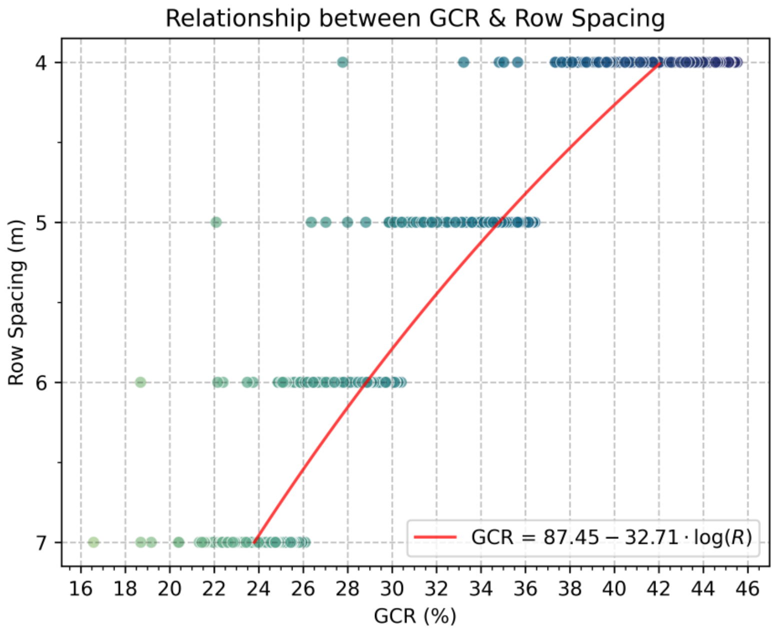

Fig. 9: Least squares fit between GCR & log(row spacing). Note axis coordinates are arranged to align with visual representation of box plots, independent variable is on vertical axis.

Tab. 6: Derived relationship between GCR and row spacing R from iterations #1 through #4.

GCR *Assuming no prior land knowledge* *Assuming row spacing R (m) is known*	
Equation	**R^2 Correlation**
$GCR = 87.45 - 32.71 \cdot \log R$ $4.0 \leq R \leq 7.0$	0.837

6.4 Example Calculation

Converting GCR to MWac can be completed as follows, based on the solar PV power plant designer's selection of:

- PV module, which has a STC capacity of M (W), length L_{module} and width W_{module} (m)
- Inverter DC/AC oversizing ratio r
- Row spacing R (for this example we have assumed this is not selected at this stage, if it was known the GCR below would be replaced with the equation in Table 6 above)

$$M_{Plant} = \frac{M}{r} \cdot \frac{GCR \cdot A_{Land}}{L_{module} W_{module}} \tag{2}$$

For example, based on a typical solar PV module capacity used in large-scale solar PV power plants as of time of writing and the author's project experience:

- $M \approx 600$ W
- $L_{module} W_{module} \approx 2$ m^2
- DC/AC oversizing ratio $r \approx 1.25$
- GCR $= 32.39\%$ (the mean from Table 5 above)

$$M_{Plant} = \frac{600}{1.25} \cdot \frac{0.3239 \cdot A_{Land}}{2} = 77.74\ \mathrm{W/m^2} \tag{3}$$

However, the author cautions the direct application of the above result. Solar PV module capacity is likely to continue to improve into the future meaning the selection of $M \approx 600$ W may not be appropriate in the future.

We also observe that repeating the above calculation with $M = 295$ W (based on the 2010 data point in Figure 1) $M_{plant} \approx 38\ \mathrm{W/m^2}$ which shows good alignment with the upper band of the values identified in the literature in Section 2.

7. Future Work & Conclusion

In this paper we have explored single-axis solar PV power plant land use requirements and derived empirical results for both the 'no prior knowledge' case and the 'row spacing knowledge' case.

Future work to expand the body of knowledge could consider the use of dual-portrait single-axis tracking systems as well as fixed-tilt systems. Variable row lengths, though uncommon, could also be investigated to improve the accuracy of the simplified logarithmic model.

The Python library used to generate the results in this section is publicly available and can be found online at the following GitHub link https://github.com/damienvermeer/sfl.

8. References

Denholm, P., & Margolis, R. M. (2008). Land-use requirements and the per-capita solar footprint for photovoltaic generation in the United States. Energy Policy, 36(9), 3531–3543. Accessed 13/10/2021. https://doi.org/10.1016/j.enpol.2008.05.035

Hernandez, R. R., Hoffacker, M. K., & Field, C. B. (2013). Land-Use Efficiency of Big Solar. Accessed 13/10/2021. https://doi.org/10.1021/es4043726

Ong, S., Campbell, C., Denholm, P., Margolis, R., & Heath, G. (2013). Land-Use Requirements for Solar Power Plants in the United States. In NREL/TP-6A20-56290. Accessed 13/10/2021. https://www.nrel.gov/docs/fy13osti/56290.pdf.

Horner, R. M., & Clark, C. E. (2013). Characterizing variability and reducing uncertainty in estimates of solar land use energy intensity. In Renewable and Sustainable Energy Reviews (Vol. 23). Accessed 13/10/2021. https://doi.org/10.1016/j.rser.2013.01.014

Wachs, E., & Engel, B. (2021). Land use for United States power generation: A critical review of existing metrics with suggestions for going forward. In Renewable and Sustainable Energy Reviews (Vol. 143). Accessed 13/10/2021. https://doi.org/10.1016/j.rser.2021.110911

Svarc, Jason. “Most Powerful Solar Panels 2021.” Clean Energy Reviews, 14 Mar. 2021, https://www.cleanenergyreviews.info/blog/most-powerful-solar-panels. Accessed 13/10/2021. Graph reproduced from data provided by Trina Solar.

ARENA’s Large-Scale Solar Program: A Look at Levelised Cost of Energy, 2018, pg 2. Accessed 13/10/2021. https://arena.gov.au/assets/2018/12/large-scale-solar-program-a-look-at-levelised-cost-of-energy.pdf.

Victoria VicMap Property cadastral maps. Accessed 2020 & 2021. https://www.land.vic.gov.au/maps-and-spatial/spatial-data/vicmap-catalogue/vicmap-property